Estimating characteristic lengths by combining direct measurements and the Kozeny-Carman relation

Quang Vu Tran, Raymond Panneton, Cong Truc Nguyen, Minh Tan Hoang, Ludovic Dejaeger, Mathieu Jouve, Valérie Marcel, Camille Perrot

JASA Express Letters

MARCH 02 2026

Estimating characteristic lengths by combining direct measurements and the Kozeny-Carman relation

Quang Vu Tran ; Raymond Panneton ; Cong Truc Nguyen ; Minh Tan Hoang; Ludovic Dejaeger; Mathieu Jouve; Valérie Marcel; Camille Perrot

JASA Express Lett. 6, 032401 (2026)
https://doi.org/10.1121/10.0042709

JASA EXPRESS LETTERS ARTICLE asa.scitation.org/journal/jel

Estimating characteristic lengths by combining direct measurements and the Kozeny–Carman relation

Quang Vu Tran,[1,2,a)] Raymond Panneton,[2,b)] Cong Truc Nguyen,[1] Minh Tan Hoang,[3] Ludovic Dejaeger,[3] Mathieu Jouve,[3] Valérie Marcel,[3] and Camille Perrot[1,c)]
[1]*Université Gustave Eiffel, Université Paris Est Creteil, CNRS, UMR 8208, MSME, Marne-la-Vallée F-77454, France*
[2]*Département de Génie Mécanique, Université de Sherbrooke, Sherbrooke, Quebec J1K 2R1, Canada*
[3]*Acoustic TechCenter Research and Development, Adler Pelzer Group, Mouzon 08210, France*

Abstract: This work revisits an indirect characterization method that exploits visco-inertial and thermal frequency response functions to estimate the macroscopic parameters of fibrous media [Panneton and Olny, J. Acoust. Soc. Am. **119**, 2027–2040 (2006); Olny and Panneton, J. Acoust. Soc. Am. **123**, 814–824 (2008)]. In practice, this method faces major challenges for highly resistive materials because the transition frequencies fall outside the measurable range of the standing-wave tube. To overcome this limitation, an alternative approach combining the equivalent characteristic-length relation derived from ultrasound measurements with a Kozeny–Carman-type relation is proposed. The methodology and its validation on resistive felts demonstrate improved estimation of viscous and thermal characteristic lengths from measurable parameters.

[Editor: Joel Mobley] https://doi.org/10.1121/10.0042709

Received: 27 December 2025 **Accepted:** 6 February 2026 **Published Online:** 2 March 2026

1. Introduction

Experimental characterization methods of acoustic porous materials exhibit a rich landscape of approaches. Among them are direct and indirect measurement techniques. Although the former are generally preferable, the latter are characterized instead by model-dependent evaluation and the requirement of assumptions to be applicable. The expected universal behavior of visco-inertial and thermal response functions is the underlying principle leveraged in many indirect characterization methods, where transport phenomena are governed by exact asymptotic limits that are connected in the complex plane with approximate but robust functions. Recent experimental developments have enabled the estimation of intrinsic macroscopic transport properties of porous materials by combining physical measurements with Bayesian inference frameworks.[1,2]

Accurately determining the intrinsic macroscopic properties of porous media is essential for understanding and predicting their acoustic behaviors.[3] Among the available experimental strategies, indirect analytical inversion methods[4–6] are widely employed for characterizing porous acoustic materials. These techniques rely on the Johnson–Champoux–Allard–Lafarge (JCAL) model[7–9] and typically invert effective dynamic properties—namely, the dynamic density ρ_{eq} and bulk modulus K_{eq}, obtained from impedance tube measurements—to infer the macroscopic intrinsic transport parameters of the material. In standard practice, the air-flow resistivity σ and open porosity ϕ are imposed as known inputs, whereas the remaining transport parameters—high-frequency tortuosity α_∞, viscous and thermal characteristic lengths Λ and Λ', and the static thermal permeability k'_0—are estimated through model inversion. Furthermore, by exploiting the low- and high-frequency asymptotic limits of the effective properties, resistivity and porosity can also be retrieved directly from dynamic measurements.[10] Nevertheless, to enhance the robustness and accuracy of the inversion procedure, directly measured parameters, generally, should be used as inputs whenever available.

Their identification with such a relatively simple characterization method brought the indirect inverse analytical approach into focus and motivated further exploration when the high-frequency behavior of the porous medium is outside the range of measurable observations. This leads to a central question regarding how several types of phenomenological conjectures can be used in combination with direct experimental techniques when the viscous f_{tv} and thermal f_{tt} transition frequencies are outside of the available measurement range (Appendix G of Ref. 11). Semi-phenomenological studies[7,9] introduced the $M = 8k_0\alpha_\infty/(\Lambda^2\phi)$ and $M' = 8k'_0/(\Lambda'^2\phi)$ dimensionless parameters and showed that they should not deviate strongly from unity for most porous structures. The Johnson–Koplik–Dashen (JKD) conjecture,

a)Email: quang-vu.tran@univ-eiffel.fr
b)Corresponding author: raymond.panneton@usherbrooke.ca
c)Email: camille.perrot@univ-eiffel.fr

$M = 8k_0\alpha_\infty/(\Lambda^2\phi) \approx 1$, was revisited by Henry *et al.*,[12] who suggested that this characteristic length Λ in the denominator could also be replaced by the characteristic length Λ', thereby leading to the formula $M_{\mathrm{KC}} = 8k_0\alpha_\infty/(\Lambda'^2\phi) \approx 1$, which they identified as a Kozeny–Carman (KC) type equation.

Advantageously, the high-frequency tortuosity α_∞ can be determined directly using ultrasound transmission measurements. This technique analyzes the propagation of ultrasound waves in a frequency range where the viscous and thermal boundary layers are much thinner than the characteristic pore size.[13,14] In this asymptotic regime, the acoustic refractive index—obtained from the phase delay between a reference pulse in air and the transmitted pulse through the sample—varies linearly with the inverse square root of frequency $f^{-1/2}$. The intercept of this linear relation with the ordinate axis yields the tortuosity α_∞, whereas its slope defines an equivalent length L_{eq}, which incorporates viscous and thermal effects according to

$$\frac{1}{L_{\mathrm{eq}}} = \frac{1}{\Lambda} + \frac{\gamma - 1}{\Lambda'\sqrt{\mathrm{Pr}}}, \tag{1}$$

where γ is the specific heat ratio and Pr is the Prandtl number of the saturating gas.

Building on the measurement principle used for tortuosity, Leclaire *et al.*[15] introduced a two-gas ultrasound transmission method in which the same porous sample is successively saturated with two gasses exhibiting markedly different physical properties—typically, air and helium. This approach enables the independent determination of the viscous and thermal characteristic lengths, Λ and Λ'. Because the two gasses have distinct values of γ and Pr, the slopes of the linear $f^{-1/2}$ dependence differ, yielding two equivalent lengths, $L_{\mathrm{eq,air}}$ and $L_{\mathrm{eq,He}}$. By solving the coupled equations derived from Eq. (1) for each gas, the viscous and thermal characteristic lengths Λ and Λ' can then be determined independently.

In this work, we demonstrate the challenges involved in estimating the viscous and thermal characteristic lengths, Λ and Λ', for highly resistive fibrous sound-absorbing materials. Our characterization strategy relies on inferring the high-frequency asymptotic behavior from ultrasound measurements performed in an air-saturated configuration. This experiment provides the high-frequency tortuosity α_∞ together with an equivalent length $L_{\mathrm{eq,air}}$, which reflects a combined contribution of the viscous characteristic length Λ and thermal characteristic length Λ'. To separate the respective viscous and thermal contributions embedded in the measured equivalent length $L_{\mathrm{eq,air}}$, we assess two phenomenological conjectures: the KC relation $[8k_0\alpha_\infty/(\Lambda'^2\phi) \approx 1]$ and JKD conjecture $[8k_0\alpha_\infty/(\Lambda^2\phi) \approx 1]$. Both are appealing because they connect the low- and high-frequency behaviors of a resistive porous structure exclusively through measurable transport parameters.

2. Materials and direct characterization methods

Two types of nonwoven recycled fibrous materials were investigated: cotton felts (F1–F4) and polyethylene terephthalate (PET) felts (B1 and B2). The cotton felts were manufactured using an airlay process from a blend consisting of 75% shoddy fibers (55% cotton and 45% PET) and 25% bicomponent fibers (PET core with a coPET sheath) by mass (mass density, 1350 g/m^2). During post-processing, the web was consolidated by thermobonding at a prescribed compression ratio,[16] where the bicomponent fibers provided thermal adhesion. The PET felts were produced from *70% PET fibers and 30% bicomponent fibers* (by mass). The web was initially formed by carding and cross-lapping, followed by mechanical reinforcement through needling, which reoriented a portion of the fibers along the thickness to create a needlefelt structure. Final consolidation was achieved by thermobonding under the selected compression ratio (Sec. 2.1 of Ref. 11). Note that this series of materials was produced using the same process as described in Sec. 2.1 of Ref. 11 but constitutes a second series that may differ slightly in composition, surface density, and compression ratio. For this reason, the characterized values reported in Ref. 11 (Tables 1 and 5) cannot be directly compared to those reported in this article (Tables 1 and 2).

The open porosity ϕ was determined using the pressure–mass method.[17] The static airflow resistivity $\sigma = \eta/k_0$ was measured at a flow velocity of 0.5 mm/s in accordance with Ref. 18, where η denotes the dynamic viscosity of air. The high-frequency ultrasound transmission technique was used to determine the tortuosity α_∞ and equivalent length in air L_{eq}.[13,14] Table 1 summarizes the results of directly measured parameters for the materials considered in this study. The reported uncertainties cover thickness measurement tolerances and statistical variability across samples. Although greater thickness may enhance precision, dimensions were constrained by the industrial process. Rigorous precautions ensured accuracy across all thicknesses, and the protocols are detailed in the supplementary material (Sec. 1).

3. Indirect analytical characterization: Limitations of characteristic-length estimations

Using the dynamic density ρ_{eq} and dynamic bulk modulus K_{eq} obtained from a three-microphone impedance tube measurement (44.4 mm in diameter),[6,19] together with the independently measured tortuosity α_∞ (Refs. 13 and 14; Table 1), the viscous and thermal characteristic lengths, Λ and Λ', can be determined via analytical inversion as[4,5]

$$\Lambda = \alpha_\infty \sqrt{\frac{2\rho_0\eta}{\omega\phi\,\mathrm{Im}(\rho_{\mathrm{eq}})\left(\rho_0\alpha_\infty - \phi\,\mathrm{Re}(\rho_{\mathrm{eq}})\right)}}, \tag{2}$$

Table 1. Direct measurements of air-saturated resistive fibrous materials, PET felts (B1 and B2) and cotton felts (F1–F4).

Samples	Thickness (mm)	Porosity ϕ	Resistivity σ (N s m^{-4})	Tortuosity α_∞	L_{eq} (μm)	Compression ratio	f_{tv} (Hz)
B1	11.1 ± 0.3	0.887 ± 0.002	47 426 ± 1699	1.089 ± 0.005	38.3 ± 4.5	1.0 ± 0.0	5250 ± 190
B2	5.1 ± 0.6	0.774 ± 0.001	161 082 ± 7561	1.175 ± 0.020	20.0 ± 4.0	2.2 ± 0.3	14 422 ± 720
F1	20.2 ± 2.7	0.945 ± 0.002	27 132 ± 561	1.023 ± 0.003	49.7 ± 1.2	1.0 ± 0.0	3406 ± 70
F2	17.0 ± 1.4	0.935 ± 0.002	48 642 ± 3523	1.035 ± 0.007	29.0 ± 3.6	1.2 ± 0.2	5972 ± 430
F3	13.3 ± 1.0	0.916 ± 0.001	84 641 ± 6965	1.042 ± 0.015	22.7 ± 3.8	1.5 ± 0.2	10 212 ± 850
F4	8.1 ± 1.1	0.860 ± 0.005	229 430 ± 12 814	1.075 ± 0.008	16.7 ± 1.5	2.5 ± 0.5	24 946 ± 1400

$$\Lambda' = \delta_t \sqrt{2}\left[-\mathrm{Im}\left(\left(\frac{K_a - K_{eq}}{K_a - \gamma K_{eq}}\right)^2\right)\right]^{-1/2}, \tag{3}$$

where $\omega = 2\pi f$ is the angular frequency, ρ_0 is the density of air at rest, $\delta_t = \sqrt{2\,\kappa/(\rho_0\, C_p\, \omega)}$ is the thermal skin depth, K_a is the adiabatic bulk modulus of air, κ is its thermal conductivity, and C_p is its specific heat at constant pressure. The reader can find the normalized dynamic density, ρ_{eq}/ρ_0, and normalized dynamic bulk modulus, K_{eq}/K_0, measured using the impedance tube in the supplementary material, Sec. 2.

To assess the validity of the analytical inversion technique applied to the materials studied here, we plot the viscous and thermal characteristic lengths, given by Eqs. (2) and (3), as functions of frequency in Figs. 1 and 2. For each material, three distinct samples were measured to illustrate spatial variability. The frequencies $f_{tv} = \sigma\phi/(2\pi\alpha_\infty\rho_0)$ and $f_{tt} = \phi\nu'/(2\pi k'_0)$ denote the transition frequencies that separate the low- and high-frequency regimes, respectively, where $\nu' = \eta/(\rho_0 \mathrm{Pr})$ is the thermal diffusivity of the saturating fluid. Here, the static thermal permeability was provided as $k'_0 = M'\phi\Lambda'^2/8$, using the measured porosity and the estimated thermal characteristic length. The coefficient $M' = 2.09$ is the dimensionless thermal shape factor, based on the average value reported for fibrous materials in Table II of Ref. 5.

As depicted in Fig. 1, the viscous characteristic length Λ exhibits a slight increase with frequency rather than the expected constant plateau, resulting in an unreliable estimation. The determination of Λ, using the analytical inversion method, should be performed in the high-frequency regime, i.e., for $f > f_{tv}$, as noted in Ref. 4. For all materials studied here except F1, the viscous transition frequency f_{tv} is relatively high as a result of its large airflow resistivities (Table 1), causing the high-frequency behavior to fall outside of the measurement range of the impedance tube used. For the lowest-resistivity material F1, although the high-frequency regime is partially captured, the measured plateau is not stable, and the estimation of Λ should, therefore, be interpreted with caution.

Similarly, the analytical inversion of the thermal characteristic length Λ' is displayed in Fig. 2. Compared to the viscous case, the results are even more unstable because of the high thermal transition frequencies f_{tt}. The complexity of this issue is exacerbated by the fact that thermal dissipation is weaker than viscous dissipation, which substantially diminishes the sensitivity of impedance tube measurements for accurately determining the equivalent bulk modulus K_{eq}. As a result, the estimation of Λ' often lacks reliability, thereby limiting its applicability for rigorous quantitative analysis. Nevertheless, a consistent trend is observed: Λ' decreases with increasing compression, as physically expected, reflecting the reduction in pore size. For comparative purposes, the constant values of Λ and Λ' estimated by the KC approach (detailed later in Sec. 4 and Table 2) are also plotted in Figs. 1 and 2. This allows for an immediate visual assessment of the fact that the indirect analytical inversions have not reached a stable plateau. It is worth noting that the tortuosity α_∞

Table 2. Comparison of the thermal Λ' and viscous Λ characteristic lengths together with their ratio Λ'/Λ for PET (B1 and B2) and cotton (F1–F4) felts obtained by four estimation methods (a) KC relation; (b) JKD conjecture; (c) L_{eq}-based estimate assuming an idealized fibrous structure, $\Lambda'/\Lambda = 2$; and (d) direct numerical simulations (Ref. 11), Sim.

	Λ' (μm)				Λ (μm)				Λ'/Λ			
Samples	(a) KC	(b) JKD	(c) $\Lambda'/\Lambda = 2$	(d) Sim	(a) KC	(b) JKD	(c) $\Lambda'/\Lambda = 2$	(d) Sim	(a) KC	(b) JKD	(c) $\Lambda'/\Lambda = 2$	(d) Sim
B1	61.5 ± 2.2	47.9 ± 7.1	94.8 ± 11.2	81.8 ± 0.7	54.2 ± 9.1	61.5 ± 2.2	47.4 ± 5.6	43.6 ± 0.4	1.13 ± 0.22	0.78 ± 0.12	2.00	1.88 ± 0.02
B2	37.1 ± 1.9	20.5 ± 4.2	49.5 ± 9.9	38.8 ± 0.2	26.8 ± 7.2	37.1 ± 1.9	24.7 ± 4.9	20.3 ± 0.1	1.38 ± 0.18	0.55 ± 0.11	2.00	1.91 ± 0.01
F1	76.6 ± 1.6	67.2 ± 2.2	123.0 ± 2.8	91.3 ± 3.0	71.7 ± 2.5	76.6 ± 1.6	61.5 ± 1.4	52.1 ± 1.7	1.07 ± 0.05	0.88 ± 0.07	2.00	1.75 ± 0.08
F2	57.6 ± 4.2	27.5 ± 3.4	71.8 ± 8.9	73.8 ± 2.2	38.0 ± 6.3	57.6 ± 4.2	35.9 ± 4.5	41.3 ± 1.2	1.52 ± 0.20	0.48 ± 0.09	2.00	1.79 ± 0.07
F3	44.3 ± 3.8	22.0 ± 3.7	56.2 ± 9.4	56.1 ± 0.6	29.9 ± 6.6	44.3 ± 3.8	28.1 ± 4.7	30.1 ± 0.3	1.48 ± 0.19	0.50 ± 0.08	2.00	1.86 ± 0.03
F4	28.2 ± 1.6	19.3 ± 2.1	41.3 ± 3.8	30.1 ± 1.2	23.2 ± 3.0	28.2 ± 1.6	20.7 ± 1.9	15.9 ± 0.6	1.22 ± 0.10	0.68 ± 0.09	2.00	1.89 ± 0.10

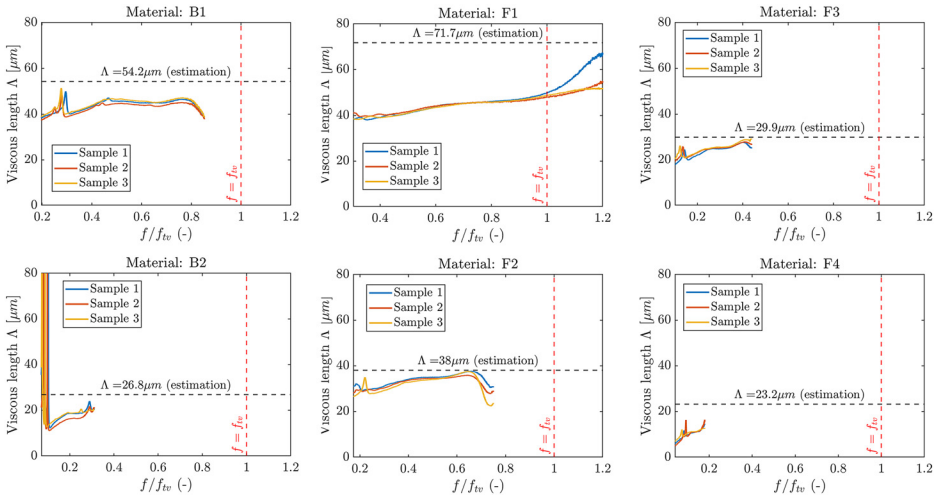

Fig. 1. Characterization of the viscous characteristic length using the analytical inversion technique. The black dashed line represents the estimate obtained using the KC relation [Eq. (4)] combined with the ultrasound measurement of L_{eq} [Eq. (1)]. The red dashed line marks the viscous transition frequency.

and the static thermal permeability k'_0 can also be estimated from acoustic measurements using the indirect method [see Eq. (11) of Ref. 4 and Eq. (12) of Ref. 5). This characterization method also fails to provide reliable estimates of the tortuosity α_∞ and static thermal permeability k'_0 (supplementary material, Sec. 1).

Overall, these observations highlight the limitations of the analytical inversion method for highly resistive fibrous materials, particularly when the relevant high-frequency regimes are inaccessible within standard impedance tube measurements. Moreover, the two-gas method for estimating characteristic lengths, as proposed by Leclaire *et al.* in 1996,[15] is relatively straightforward to implement experimentally, relying only on standard ultrasound and vacuum equipment. However, it requires that the saturating gasses completely fill the pore volume of the sample to ensure reliable measurements. In the present study, the measurements performed with helium did not yield consistent results and produced unrealistically large values (supplementary material, Sec. 2), most likely caused by incomplete gas saturation within the fibrous samples. As a result, only the equivalent length $L_{eq,air}$ measured in air could be used (Table 1), preventing the independent estimation of Λ and Λ'.

As a result of the limitations in estimating the viscous and thermal characteristic lengths of highly resistive fibrous materials, discussed above, an alternative estimation strategy is presented in Sec. 4.

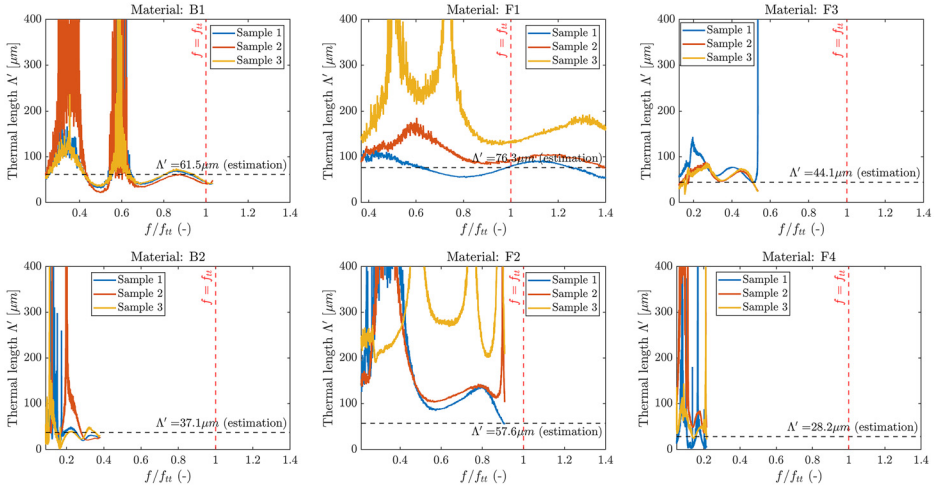

Fig. 2. Characterization of the thermal characteristic length using the analytical inversion technique. The black dashed line represents the estimate obtained using the KC relation [Eq. (4)] combined with the ultrasound measurement of L_{eq} [Eq. (1)]. The red dashed line marks the thermal transition frequency.

4. Alternative estimation approach based on the KC relation

Several approaches exist in the literature to relate the permeability of a porous medium to its microstructural characteristics. One widely used method is based on the KC relation.[20–22] This semi-empirical relation estimates the permeability of granular materials from the inverse of the specific surface area (pore surface per unit solid volume) and porosity. The corresponding KC formulation was subsequently extended to foams and fibrous materials.[23,24] In addition, Walsh and Brace,[25] Berryman and Blair,[26] and Schwartz *et al.*[27] incorporated the electrical formation factor F to account for pore connectivity and tortuosity in KC type relations. In these formulations, the formation factor is related to the tortuosity of the porous medium, typically through $F = \alpha_\infty/\phi$, which allows the permeability to be expressed in terms of the porosity ϕ, tortuosity α_∞, and the thermal characteristic length Λ'. This approach leads to the form employed by Henry *et al.*,[12] $\sigma = 8\alpha_\infty\eta/(\phi\,\Lambda'^2)$.

This empirical KC relation, linking the resistivity to other measurable properties of a porous material, thus, can provide an estimate of the thermal characteristic length such that

$$\Lambda' = \sqrt{\frac{8\,\alpha_\infty\,\eta}{\phi\,\sigma}}. \tag{4}$$

Once Λ' is determined, the viscous characteristic length Λ can be obtained by combining it with the equivalent length L_{eq} through Eq. (1).

5. Discussion and conclusions

Table 2 compares the viscous (Λ) and thermal (Λ') characteristic lengths obtained using the four estimation methods:

(1) The determination of Λ' from the KC conjecture or relation [Eq. (4)], combined with an ultrasound measurement of L_{eq} [Eq. (1)] to obtain Λ.
(2) The determination of Λ from the JKD conjecture, $\Lambda = \sqrt{(8\,\alpha_\infty\,\eta)/(\phi\,\sigma)}$ (in which it is implicitly assumed that the M factor is equal to one), together with an ultrasound measurement of L_{eq} [Eq. (1)], to obtain Λ'.
(3) The determination of Λ' and Λ is achieved by solving Eq. (1) for $\Lambda'/\Lambda = 2$ using experimental values of L_{eq}. This ratio of 2 is a theoretical result obtained by Allard and Champoux[28] from a single dilute fiber.
(4) Direct numerical simulations by Tran *et al.*[11]

In what follows, we discuss the characterized and computationally obtained values of the viscous Λ and thermal Λ' characteristic lengths:

(1) The KC and JKD conjectures offer different perspectives on the microscopic foundations of macroscopic transport in porous media. The KC-based approach is inherently more empirical as it relies primarily on a sequence of standard laboratory measurements—namely, porosity, resistivity, and ultrasound-derived tortuosity.[23] Conversely, the JKD conjecture originates from a quest for a theoretical framework that integrates exact asymptotic mathematical limits with numerical simulations.[7]
(2) All approaches yield consistent overall trends, showing a systematic decrease in Λ and Λ' with increasing compression ratios, as expected from the corresponding reductions in pore sizes. However, some discrepancies are observed between the different estimation methods.
(3) In this study, the second estimation method, based on the JKD conjecture, does not seem applicable because it violates the inequality $\Lambda' \geq \Lambda$, which reflects the fact that in porous materials, the thermal diffusion path (Λ') is expected to be larger than (or at least equal to) the viscous path (Λ).
(4) The inappropriateness of the JKD conjecture in the present case can be explained by the simplifying assumption $M = 1$. As discussed in Ref. 7, the dimensionless factor M accounts for the influence of pore connectivity and deviations from the ideal capillary-tube geometry. From Table 1 of Ref. 29, M typically varies from 1.4 to 2.5 (experimental results), which is comparable to the values reported by Johnson *et al.*[7] (Sec. 3) found from network simulations (from 1.6 to 2.0). The results obtained by either experiments[29] or simulations,[7] therefore, suggest that assuming $M = 1$ may lead to an overestimation of Λ. Alternatively, the KC conjecture, when combined with the ultrasonic measurement of L_{eq}, allows the dimensionless factor M to be directly evaluated for each material. The values obtained are F1 ($M = 1.11$), F2 ($M = 2.26$), F3 ($M = 2.15$), F4 ($M = 1.45$), B1 ($M = 1.26$), and B2 ($M = 1.88$). These values fall within the ranges reported by Baker[29] and Johnson *et al.*.[7] In other words, M should be close to unity, but the strict equality $M = 1$ is too strong for the relationship (JKD conjecture) to be used as an accurate predictor.
(5) For all materials, the KC-based results lead to ratios Λ'/Λ ranging between 1.0 and 1.5, which agree relatively well with values typically reported for fibrous porous media. Our numerical simulations reveal ratio values ranging between 1.75 ± 0.08 and 1.91 ± 0.01 (Ref. 11).
(6) Conversely, the KC formulation provides a more physically consistent estimate of the characteristic lengths (by respecting the $\Lambda' \geq \Lambda$ constraint) than the JKD conjecture does for these fibrous materials.
(7) Assuming that the porous material to be characterized is a fibrous structure ($\Lambda'/\Lambda \simeq 2$), the third approach provides fairly good estimates of the characteristic lengths (Λ and Λ').

(8) It is also noteworthy that the inequality $\Lambda'_{KC} \leq \Lambda'_{Sim}$ holds (see, also, the supplementary material, Sec. 5).
(9) Overall, in comparison with the numerical results reported by Tran *et al.*,[11] the values obtained using the KC approach show better overall agreement than those from the JKD approach and the case $\Lambda'/\Lambda = 2$. Although some discrepancies are still present, the KC-based predictions recover the correct order of magnitude found in the numerical models. This close agreement further corroborates the suitability of employing the KC relation, together with ultrasound measurements of $L_{eq,air}$, as a robust method for determining Λ and Λ' in fibrous porous media. The reader is referred to Sec. 6 of the supplementary material for a detailed comparison of the method's errors against the numerical solutions.
(10) Finally, the identification of characteristic lengths using the proposed KC approach yields a high degree of consistency when reconstructing intrinsic frequency-dependent quantities—specifically the dynamic density ρ_{eq} and bulk modulus K_{eq}—as well as the predicted sound absorption coefficient at normal incidence. As shown in the supplementary material (Sec. 2), these estimates align closely with experimental measurements, confirming the robustness of the KC relation combined with ultrasound measurements of $L_{eq,air}$ for characterizing these fibrous materials.

Supplementary Material

See the supplementary material for additional information on (1) the direct characterization methods that were followed during the course of this work; (2) the comparisons between experimentally determined and modeled frequency-dependent effective properties, including the normalized effective density ρ_{eq}/ρ_0, the normalized effective bulk modulus K_{eq}/K_0, and the sound absorption coefficient at normal incidence; (3) the limitations of the analytical inversion techniques for estimating the tortuosity α_∞ and the static thermal permeability k'_0; (4) the ultrasonic measurements performed with air and helium show that helium saturation did not yield consistent results and led to unrealistically large values; (5) the evaluation of the finite length effect of the pores on the estimates of Λ'; (6) comparison of the three estimation methods compared with numerical simulations.

Acknowledgements

The authors are pleased to thank two anonymous reviewers for their valuable comments and suggestions that helped improve the manuscript. This work was part of a project sponsored by (1) the Association Nationale Recherche Technologie (France) and was accomplished under a research collaborative agreement with Adler Pelzer Group under ref. ANRT Cifre n° 2020-0122 (Ref. EIFFEL 2021-00120); (2) a cooperative agreement between Université Gustave Eiffel, Adler Pelzer Group, and Université de Sherbrooke under Ref. Eiffel 2024-00043; as well as (3) PUI SEVille France 2030 (project PolyFib). Q.V.T. also acknowledges the financial support of Labex MMCD. Labex MMCD benefits from a French government grant managed by ANR within the framework of the national program investments for the Future ANR-11-LABX-022-01. R.P. acknowledges the financial support of the Natural Sciences and Engineering Research Council of Canada (NSERC Ref. RGPIN-2018–06113). The authors also wish to thank Mecanum Inc. for providing access to its acoustic material characterization laboratory. The authors are grateful to Jean-Yves Curien for helpful discussions.

Author Declarations

Conflict of Interest

The authors have no conflicts to disclose.

Data Availability

The data that support the findings of this study are available from the corresponding author upon reasonable request.

References

[1]M. Niskanen, J.-P. Groby, A. Duclos, O. Dazel, J. C. Le Roux, N. Poulain, T. Huttunen, and T. Lähivaara, "Deterministic and statistical characterization of rigid frame porous materials from impedance tube measurements," J. Acoust. Soc. Am. **142**(4), 2407–2418 (2017).
[2]J. Cuenca, P. Göransson, L. De Ryck, and T. Lähivaara, "Deterministic and statistical methods for the characterisation of poroelastic media from multi-observation sound absorption measurements," Mech. Syst. Sig. Process. **163**, 108186 (2022).
[3]L. L. Beranek, "Acoustic impedance of porous materials," J. Acoust. Soc. Am. **13**(3), 248–260 (1942).
[4]R. Panneton and X. Olny, "Acoustical determination of the parameters governing viscous dissipation in porous media," J. Acoust. Soc. Am. **119**(4), 2027–2040 (2006).
[5]X. Olny and R. Panneton, "Acoustical determination of the parameters governing thermal dissipation in porous media," J. Acoust. Soc. Am. **123**(2), 814–824 (2008).
[6]O. Doutres, Y. Salissou, N. Atalla, and R. Panneton, "Evaluation of the acoustic and non-acoustic properties of sound absorbing materials using a three-microphone impedance tube," Appl. Acoust. **71**(6), 506–509 (2010).
[7]D. Johnson, J. Koplik, and R. Dashen, "Theory of dynamic permeability and tortuosity in fluid-saturated porous media," J. Fluid Mech. **176**, 379–402 (1987).
[8]Y. Champoux and J.-F. Allard, "Dynamic tortuosity and bulk modulus in air-saturated porous media," J. Appl. Phys. **70**(4), 1975–1979 (1991).

[9]D. Lafarge, P. Lemarinier, J.-F. Allard, and V. Tarnow, "Dynamic compressibility of air in porous structures at audible frequencies," J. Acoust. Soc. Am. **102**(4), 1995–2006 (1997).
[10]L. Jaouen, E. Gourdon, and P. Glé, "Estimation of all six parameters of Johnson-Champoux-Allard-Lafarge model for acoustical porous materials from impedance tube measurements," J. Acoust. Soc. Am. **148**(4), 1998–2005 (2020).
[11]Q. V. Tran, C. Perrot, R. Panneton, M. T. Hoang, L. Dejaeger, V. Marcel, and M. Jouve, "Effect of polydispersity on the transport and sound absorbing properties of three-dimensional random fibrous structures," Int. J. Solids Struct. **296**, 112840 (2024).
[12]M. Henry, P. Lemarinier, J. F. Allard, J. L. Bonardet, and A. Gedeon, "Evaluation of the characteristic dimensions for porous sound-absorbing materials," J. Appl. Phys. **77**(1), 17–20 (1995).
[13]J. F. Allard, B. Castagnede, M. Henry, and W. Lauriks, "Evaluation of tortuosity in acoustic porous materials saturated by air," Rev. Sci. Instrum. **65**(3), 754–755 (1994).
[14]A. Moussatov, C. Ayrault, and B. Castagnède, "Porous material characterization—Ultrasonic method for estimation of tortuosity and characteristic length using a barometric chamber," Ultrasonics **39**(3), 195–202 (2001).
[15]P. Leclaire, L. Kelders, W. Lauriks, M. Melon, N. Brown, and B. Castagnède, "Determination of the viscous and thermal characteristic lengths of plastic foams by ultrasonic measurements in helium and air," J. Appl. Phys. **80**(4), 2009–2012 (1996).
[16]B. Castagnède, A. Moussatov, and V. Tarnow, "Parametric study of the influence of compression on the acoustical anisotropy of automotive felts," C. R. Acad. Sci., Ser. IIb: Mec. **329**(4), 295–301 (2001).
[17]Y. Salissou and R. Panneton, "Pressure/mass method to measure open porosity of porous solids," J. Appl. Phys. **101**(12), 124913 (2007).
[18]M. R. Stinson and G. A. Daigle, "Electronic system for the measurement of flow resistance," J. Acoust. Soc. Am. **83**(6), 2422–2428 (1988).
[19]T. Iwase, Y. Izumi, and R. Kawabata, "A new measuring method for sound propagation constant by using sound tube without any air spaces back of a test material," in *INTER-NOISE and NOISE-CON Congress and Conference Proceedings*, Christchurch, New Zealand (16 October 1998) (Institute of Noise Control Engineering, Wakefield, MA, 1998), Vol. 1998, pp. 1265–1268.
[20]J. Kozeny, "Capillary conduction of water in the soil," Sitz.-Ber. K. Akad. Wiss. **136**, 271–309 (1927).
[21]P. C. Carman, "Fluid flow through granular beds," Trans. Inst. Chem. Eng. London **15**, 150–156 (1937).
[22]W. D. Carrier, "Goodbye, Hazen; hello, Kozeny-Carman," J. Geotech. Geoenviron. Eng. **129**(11), 1054–1056 (2003).
[23]M. T. Pelegrinis, K. V. Horoshenkov, and A. Burnett, "An application of Kozeny–Carman flow resistivity model to predict the acoustical properties of polyester fibre," Appl. Acoust. **101**, 1–4 (2016).
[24]P. Kumar and F. Topin, "State-of-the-art of pressure drop in open-cell porous foams: Review of experiments and correlations," J. Fluids Eng. **139**(11), 111401 (2017).
[25]J. B. Walsh and W. Brace, "The effect of pressure on porosity and the transport properties of rock," J. Geophys. Res. [Solid Earth] **89**(B11), 9425–9431, https://doi.org/10.1029/JB089iB11p09425 (1984).
[26]J. G. Berryman and S. C. Blair, "Kozeny–Carman relations and image processing methods for estimating Darcy's constant," J. Appl. Phys. **62**(6), 2221–2228 (1987).
[27]L. M. Schwartz, N. Martys, D. P. Bentz, E. J. Garboczi, and S. Torquato, "Cross-property relations and permeability estimation in model porous media," Phys. Rev. E **48**, 4584–4591 (1993).
[28]J.-F. Allard and Y. Champoux, "New empirical equations for sound propagation in rigid frame fibrous materials," J. Acoust. Soc. Am. **91**(6), 3346–3353 (1992).
[29]S. R. Baker, "Sound propagation in a superfluid helium filled porous solid: Theory and experiment," Ph.D. thesis, University of California, Los Angeles (UCLA), Los Angeles, CA, 1986.